Ion Beam Modification of Materials, Canberra, AUS, Feb 5-10, 1995, ver. 01/27/95 8:12 AM

The Use of Low Energy, Ion Induced Nuclear Reactions for Proton Radiotherapy Applications*

K.M. Horn[1], B. Doyle[1], M.N. Segal[2], R.W. Hamm[3], R.J. Adler[4], and E. Glatstein[5]
1) Sandia National Laboratories, 2) Dept. of Otolaryngology,University of New Mexico Medical School, 3) Accsys Technology Inc., 4) North Star Research Corp., 5) Dept. of Rad. Oncology, University of Texas Southwest Medical Center

Medical radiotherapy has traditionally relied upon the use of external photon beams and internally implanted radioisotopes as the chief means of irradiating tumors. However, advances in accelerator technology and the exploitation of novel means of producing radiation may provide useful alternatives to some current modes of medical radiation delivery - with reduced total dose to surrounding healthy tissue, reduced expense, or increased treatment accessibility. This paper will briefly overview currently established modes of radiation therapy, techniques still considered experimental but in clinical use, innovative concepts under study that may enable new forms of treatment or enhance existing ones. The potential role of low energy, ion-induced nuclear reactions in radiotherapy applications is examined specifically for the 650 keV d(^{3}He,p)^{4}He nuclear reaction. This examination will describe the basic physics associated with this reaction's production of 17.4 MeV protons and the processes used to fabricate the necessary materials used in the technique. Calculations of the delivered radiation dose, heat generation, and required exposure times are presented. Experimental data is also presented validating the dose calculations. The design of small, lower cost ion accelerators, as embodied in 'nested'-tandem and radio frequency quadrupole accelerators is examined, as is the potential use of high-output ^{3}He and deuterium ion sources. Finally, potential clinical applications are discussed in terms of the advantages and disadvantages of this technique with respect to current radiotherapy methods and equipment.

DISCLAIMER

* This work performed, in part, at Sandia National Laboratories supported by the U.S. Department of Energy under Contract DE-AC04-94AL8500.

Background

Ideally, the aim of medical radiation therapy is to deliver a lethal dose of radiation to a clearly defined region of diseased tissue while inflicting little or no radiation damage on surrounding healthy tissue. However, the delivery of radiation to the diseased tissue almost always involves transport of the incident radiation across healthy tissue. It has been stated in the medical literature that, "... large tumors are less likely to be cured at doses of radiation that are still within the tolerance of adjacent normal tissue. Normal tissue sparing is enhanced when (a) the volume of irradiated normal tissue is reduced and (b) the biologic effect on tumor cells is greater than that on surrounding normal cells. These two factors must be optimized to improve the probability of an uncomplicated cure" [1].

The most widely accepted and utilized form of radiation treatment is external beam radiotherapy. This term applies to the use of x-rays or gamma rays to deposit energy at the site of a tumor. Beams of x-rays are usually produced by linear electron accelerators or x-ray tubes, while the decay of elements such as radium, uranium or cobalt-60 serve as sources of gamma radiation. The depth of irradiation is controlled through the setting of the x-ray beam energy or selection of the gamma ray source. As illustrated in figure 1, significant damage is delivered over the entire length of the radiation's path. Controlling the balance between the damage delivered to the tumor and that done to intervening healthy tissue is critical in performing the therapy. Exploiting what is termed the dose-response effect, (i.e. the ability of healthy cells to recover from radiation damage more quickly than cancerous cells), repeated exposures at sub-lethal doses are delivered to both the tumor and the surrounding healthy tissue in a timed sequence such that, owing to the dose-response effect, the accumulated damage at the tumor exceeds that of the healthy tissue. Thus, although the radiation is broadly delivered, the damage induced is more localized owing to the differences in recovery times of the exposed tissues.

A higher degree of damage localization is often achieved through the use of radioactive implants, a treatment called internal radiotherapy. Specific clinical procedures based upon this concept are referred to as brachytherapy, interstitial irradiation, and intracavitary irradiation. In this procedure, radioisotopes are physically inserted at the site of the tumor. The irradiated volume depends upon the range of the decay products of the implanted radioisotopes and the size of the region over which the material is implanted. This procedure most often requires the patient to remain in the hospital for the length of the treatment, normally a few days, until the implanted radioisotopes are removed.

One new technique being explored in radiation therapy is intra-operative irradiation; in this procedure, the site of the surgically removed tumor and the surrounding tissue are irradiated with a large dose of external radiation while exposed during surgery. In this way, isolated cancer cells still remaining after removal of the main body of the tumor, are killed in situ. One problem with this technique resides in the common need to transport the patient from the sterilized environment of the surgical theater to the

radiation facilities of the hospital. A suitably compact radiation source for in-operating room irradiation would greatly facilitate this technique.

In cases of inoperable tumors, such as brain and eye tumors, a number of techniques referred to as particle beam radiation therapy have been developed and performed clinically. Such techniques use beams of energetic neutrons, pions, and heavy ions to externally irradiate surgically inaccessible tumors. The most widely used form of this technique is called proton radiotherapy; worldwide, nineteen facilities exist which have treated patients with this technique and fourteen new facilities are currently proposed or under construction [2]. First proposed by Robert Wilson in 1946 [3], proton radiotherapy exploits the enhanced energy deposition manifest at the end of range of energetic ion beams (i.e. the Bragg peak) as a means of preferentially depositing energy at a tumor site. In practice, synchrotron- or cyclotron-produced high energy proton beams, with energies of 50 to 250 MeV, are precisely targeted into the immobilized patient along an incident path selected to minimize damage to intervening sensitive organs or tissue. The energy of the incident beam is selected so that the protons come to rest at or near the tumor. Variations in the depth of penetration are accomplished using devices called "phantoms" or boluses which tailor the range of the initially monoenergetic incident beam before it enters the patient. As shown in figure 1, the damage done along the incident path of the beam can be as little as 30% of that delivered to the site of the tumor. However, even with this reduction in dose to healthy tissue, the incidental radiation damage limits the deliverable dose for any single exposure and often requires the use of either multiple incident paths in a single radiation treatment, or fractionated treatments at sub-lethal doses over multiple sessions, again relying on differing dose-response effects. Proton radiotherapy requires precise radiation transport and targeting calculations, and also the ability to maintain rigid control of the patient's position and/or the incident beam trajectory during treatment.

Even higher localization of irradiation is attempted with a technique called Neutron Capture Therapy, first proposed in the 1930s [4]. Boron neutron capture therapy (BNCT) involves the selective introduction of boron-10 to a tumor site, via administration of chemically tailored ^{10}B-containing compounds which preferentially bind to tumor cells. Once the tumor is "doped" with boron-10, the patient is exposed, either intra-operatively or externally, to thermal (<1eV) or epithermal (1eV - 10 keV) neutrons. These neutrons have only modest interaction with the surrounding boron-free, healthy tissue, but can induce the $^{10}B(n,\alpha)^{7}Li$ nuclear reaction in the ^{10}B-doped tumor. This reaction produces lithium and helium fission fragments with a shared energy of 2.3 MeV, and a range in tissue of approximately 10 microns; this is comparable to the dimension of a single mammalian cell. Thus, localization of damage is achieved by producing the most damaging radiation at the site of the tumor and the spatial extent of the damage is controlled by the range of the reaction products.

Other research has combined chemical and radiological effects through use of radiosensitizer drugs, which enhance a tumor's susceptibility to radiation damage, and radioprotectors that conversely increase the radiation tolerance of normal tissue. Related radiobiological effects based upon thermal changes in

radiosensitivity (hypothermia), and the oxygen-dependence of radiation damage (hypoxia), are also being investigated for their potential in selectively altering the susceptibility of tissue to radiation. Radiation exposures introduced even at the molecular level are being studied via the use of radiolabeled antibodies which preferentially deliver radiation to the tumor in a technique termed radioimmunotherapy.

Introduction

The continuing trend in the development and enhancement of radiation therapy techniques is toward greater spatial control of the induced damage around tumors and reduced exposure of healthy tissue. Convoluted with this clear clinical objective, however, are the pragmatic constraints imposed by the need for any new techniques or equipment to be more effective, affordable, accessible, and produce less medical waste than current techniques. Within this framework, we present a description of a new concept for the production and delivery of energetic protons for use in radiotherapy; it is based upon the fact that low energy, ion-induced nuclear reactions can produce highly energetic radiation products suitable for use in tumor irradiation. By employing specially fabricated needles as evacuated conduits to deliver beams of energetic ions to selected target materials sealing the end of the needle, ion beam-induced nuclear reactions can be generated at the needle tip which emit reaction-specific radiation products.

The $d(^3He,p)^4He$ nuclear reaction produces energetic protons suitable for radiotherapy applications. In this reaction, the collision of a 650 keV ^3He nucleus with a deuterium nucleus can result in a nuclear reaction which produces ^4He, and a proton with energies that vary from 13.6 MeV at 90° (lab frame) up to 17.4 MeV at 0°. The tip of the needle, under ion exposure, constitutes a highly localized, switchable source of radiation. The incident, low energy ion beam is stopped in the needle walls. The irradiated volume is strictly limited to the range of the reaction products and the placement of the needle.

Two separate implementations of the ion-induced nuclear radiotherapy (hereafter referred to as INRT) concept are shown schematically in Figure 2. In its internal usage, which we will refer to as μINRT, the needle tip is used to produce a point-source of radiation at the tumor site. In this mode, which is analogous to a switchable, intensity-adjustable form of brachytherapy, it is envisioned that the INRT-needle is inserted to the site of a tumor in the same manner that a biopsy needle is inserted into a patient to sample the tumor. Once positioned, the axis of the incident low energy ion beam and the insertion vector of the INRT needle are made coincident by adjusting electrostatic steering of the low energy ion beam or by re-orienting the entire accelerator assembly on its own three-axis frame; two types of compact, lightweight (several hundred pound) accelerators suitable for INRT are described later in this article. The ion beam is directed down the evacuated needle where it strikes the needle tip producing the radiation products. The radiation is confined to a pre-determined region about the tip of the needle, defined by the range of the reaction products in tissue. Since the INRT-needle delivers the low energy ion beam to the

tumor site without any radiation damage to the surrounding tissue, the deliverable dose is not limited by incidental dose to healthy tissue.

In the external mode of usage, referred to as topical INRT (figure 2b), a broad swathe of radiation is produced by positioning the needle-tip some distance back from the exposed treatment surface; the intervening air gap permits the reaction products to spatially diverge with marginal energy loss before striking the larger target area. A simple Plexiglas shroud surrounding the external needle (tube) confines the radiation products to the intended exposure site and the area of irradiation is readily defined through use of masking materials only millimeters thick.

Ion Induced Nuclear Radiotherapy

i. The 650 keV d(^{3}He,p)^{4}He Nuclear Reaction

The total yield of energetic protons from such an ion-induced nuclear reaction can be given in its simplest form, for a target of uniform deuterium concentration, as:

$$Y = N_i \cdot C_d \cdot \Sigma\sigma(E)\delta x$$

The number of incident ions, N_i, is usually measured in terms of the total electrical charge deposited on the target by the ion beam. For a beam of singly-ionized ^{3}He ions, N_i is simply the total charge collected on target divided by the charge per ion (1.6×10^{-19} Coulombs). A 1 microCoulomb (μC) ion exposure therefore corresponds to $N_i = 6.25\times10^{12}$ incident ^{3}He nuclei.

C_d is the deuterium concentration in the target, which is uniform in this case. Metal matrices such as titanium, zirconium, erbium and scandium have been shown to maintain stable hydrogen (and deuterium) concentrations of 1.16×10^{23} deuterium/cm^3, or a stoichiometry of TiD_2, for example [5].

$\sigma(E)$, the reaction's energy-dependent total cross section, is reported for ^{3}He energies up to 2.5 MeV by Möller and Besenbacher [6]. The cross section for this reaction is quite broad with a peak of 0.825 barn at about 650 keV. A slightly higher incident ^{3}He energy of 800 keV is used in order to increase the thick target proton yield from the reaction. $\sigma(E)$ is converted to a depth-dependent $\sigma(x)$ by using the energy-dependent stopping power (dE/dx) of the incident ^{3}He ion in the target to convert the energy-dependence of the published cross section to a corresponding depth-dependence specific to the target and incident beam energy. The total integrated cross section for an 800 keV ^{3}He ion in TiD_2, over its full range of 1.9 microns in TiD_2, is 6.7×10^{-29} cm^3.

The total yield of 17.4 MeV protons resulting from a 1μC exposure of a TiD_2 INRT needle to an 800 keV ^{3}He ion beam is then calculated to be, $Y = 4.85\times10^7$ protons/μC ^{3}He.

Since 17.4 MeV protons have a range of 3.1 millimeters in tissue [7], the irradiated volume is 0.125 cm^3. Applying the definition of dose as "the amount of energy imparted to matter by ionizing

particles per unit mass of irradiated material" [6], the delivered radiation dose per 17.4 MeV proton to the 0.125 cm^3 exposed volume of tissue, with a density of 1.0 g/cm^3, is 2.2×10^{-6} rads/proton. Multiplying this dose rate per proton by the number of protons produced per incident μC yields a total dose delivery rate of 108 rads/μC. Thus, a 1.0 microamp ^3He ion beam directed onto a TiD_2 INRT needle delivers roughly 100 rad/sec, or 1 Gy/sec, to the irradiated volume.

However, in order to include both the $1/r^2$ dependence of the energy deposition and the end-of-range Bragg peak in the proton dose deposition curve, a computer simulation of the proton energy loss through individual volume elements within the exposed volume was performed. This calculation uses a differential form for the radiation dose delivered by the protons:

$$\text{dose}(r,\theta,\phi) = (dE/dr)/(4\pi\rho r^2) \quad \text{or} \quad .618\ dE/dr(MeV/mm)/r^2(mm^2) \quad \text{in Gy/}\mu\text{C } ^3\text{He}, \qquad \text{eq. 1}$$

where dE/dr is the stopping power of the protons in tissue. The computer simulation assumes a water target which has the same density as tissue. Parametric equations for the proton Range vs. Energy (i.e. $R= f_R(E)$) and Energy vs. Range (i.e. $E=f_E(R)$) calculations were made by curve-fitting Range-Energy data generated by the TRIM program. Using the parametric forms for these equations, an analytical representation for the proton energy as a function of position (r,θ,ϕ) is found:

$$E(MeV) = f_E(f_R(E_0(\theta)) - r)) \qquad \text{eq.2}$$

where

$$f_R(E) = (10^{2(.76E-2.09)} + 10^{2(1.73E-1.66)})^{1/2} \quad \text{and} \quad 1/f_E(R) = (10^{-3(1.30R+2.70)} + 10^{-3(.574R+.957)})^{1/3} \qquad \text{eq.3}$$

with E and E_0 in MeV; R and r are in millimeters.

The initial proton energy E_0, which is a function of emission angle θ, can also be represented parametrically:

$$E_0(\theta) = 17.228 \exp(-(\theta(\text{degrees})/255)^{1.8}) \text{ in MeV.} \qquad \text{eq.4}$$

This expression takes into account a small energy loss in the TiD_2 target foil. The stopping power, dE/dr, was determined by numerically differentiating eq. 2.

ii. μINRT Radiation Field

Figure 2a displays a three dimensional rendering of the radiation pattern, in Gray/sec, resulting from an INRT exposure using a 1 μA, 800 keV ^3He ion beam incident on a TiD_2-tipped needle. The volume element used in calculating the radiation dose is 50 microns on edge. As is apparent, the $1/r^2$ dependence of the radiation intensity dominates the pattern, though the Bragg peak effects are also visible. The baseline, or minimum, deposition within the irradiated area is 0.7 Gy/sec. Figure 3 illustrates the time evolution of the radiation damage pattern for a cross-section of the radiation pattern. Exposures as short as 20 seconds deliver a minimum of 15 Gy to the entire treatment volume. The results of the computer calculations are compared to measurements made with a prototype INRT needle in figure 4. The energy

deposited (or dose delivered) by energetic protons transmitted through water were measured using a surface barrier detector immersed in the water at various distances from the needle tip. Including the thickness of the detector's waterproof sleeve and surface metallization in the calculation, the results indicate very good agreement between the computer simulation and the experimentally measured dose.

iii. Topical INRT Radiation Field

For use in dermatological or intra-operative procedures, a broader, more uniform dose distribution can be achieved by displacing the INRT needle back from the target so as to allow the product radiation to diverge from the needle tip. Increasing the distance from the needle to the target is done at the cost of reduced dose rate, unless the incident ion beam current is raised to compensate for this by increasing the rate of radiation production. Since the topical INRT needle is not in physical contact with any tissue and the 'needle' diameter is large (1") allowing the power density to be moderated by increasing the beam spot diameter, the beam current can be increased to attain higher radiation output yields. Figure 2b displays a three dimensional rendering of the radiation pattern, in Gray/sec, resulting from an INRT exposure using a 1 milliamp, 800 keV ^{3}He ion beam incident on a TiD_2-tipped needle. The 1" diameter 'needle' is displaced from the target by 6". The volume element used in calculating the radiation dose is 100 microns on edge. The baseline radiation dose rate in this implementation is 0.1 Gy/sec.

iv. Thermal Effects

The dissipation of heat produced by the incident ^{3}He ion beam impacting the needle-end is also a concern in evaluating possible effects on surrounding healthy tissue. For the purpose of estimating the local temperature rise due to this technique, the heat transfer process is approximated by considering the treatment area as imbedded in a large mass with the same stoichiometry and thermal conductivity as muscle tissue. This, of course only applies to the μINRT application; in the topical treatment no needle contact with the tissue occurs so heating is irrelevant except for the target film's integrity. Heat, (corresponding to the stopping of a 1 μA ^{3}He ion beam in the needle-end), is introduced continuously over a 100 second exposure time at the center of this volume and removed only by conduction through the medium. The temperature at the outer boundary of the irradiated volume would increase by approximately 12 °C during the 70 Gy exposure and decrease to less than a 5 °C elevation in temperature above ambient within 40 seconds after the end of the exposure. This conservative estimate assumes only a static thermal mass, and excludes heat removal by the INRT needle and the local circulatory system. The temperature increase above ambient, due to the radiation delivery is shown in figure 5 for positions 5mm and 3mm from the needle tip and at the tip. Moderate elevation of the local temperature in and around the tumor may even be a desirable effect. It has been observed that the elevation of temperature increases the radiosensitivity of tumors; after one hour of heating at 43°C, the radiosensitivity of certain tumors has

increased by factors of 3 to 4 [8]. Thus, the heat generated by the μINRT technique may be useful in enhancing its effectiveness.

Accelerator Technologies

The development of smaller, more efficient radiation sources has been one result of the technological advances of the last decade. Compact radio frequency quadrupoles, linear accelerators, and tandem accelerator systems have been designed and built for purposes ranging from explosives detection in luggage [9], to rocket-borne strategic defense, to radioisotope production for use in positron emission tomography [10]. Compact, efficient ion accelerators, suitable for implementation of INRT are already commercially available. Detailed descriptions of two such accelerator designs are given below.

i. Radio Frequency Quadrupole

Prior to development of a high-frequency radio-frequency quadrupole (RFQ) linac by scientists at the Los Alamos National Laboratory in 1980, [11] existing ion linacs were all large accelerators used at physics research facilities. The RFQ is essentially an rf-driven quadrupole focusing channel that is perturbed to provide an axial accelerating potential by periodic modulation of the four pole tips [12, 13]. Through tailoring of the modulation to gradually turn on the axial field component, [14] one can capture most of a low energy beam injected into the structure in the rf accelerating field. Within the constraint imposed by rf sparking between adjacent pole tips, the RFQ designer has a large latitude in varying the input energy, vane modulation, and bore diameter to accommodate large or small beam currents, with accompanying changes in the beam transmission and rf power requirements. For low beam current applications, the RFQ can be designed to have high transmission, low rf power and relatively short length, even for MeV output energies, if a high operating frequency is used. These characteristics have been exploited in the design of a compact linac system for proton radiotherapy using low energy ^{3}He ion induced nuclear reactions. This compact system is capable of delivering 10 μA of $^3He^+$ ion beam at 800 keV output energy with a beam spot diameter of 1 mm. It is only 60 cm in length and requires an input ac power of only 1500 watts. At the cost of higher power consumption, the same system can be used to deliver up to 1 milliamp at 800 keV with a beam spot diameter of 2 cm.

Because INRT needs only a fixed output energy, the RFQ system offers several advantages for this application. It is simple to operate, and produces no radiation during its operation because of the low rf accelerating voltage. The duoplasmatron ion source used to produce the $^3He^+$ beam has a small emittance at the low currents required for INRT applications, making the output beam from the RFQ easy to focus to a beam spot as small as 1.0 mm. The ac power required is standard 110V. Accelerator maintenance is minimal, because there are no moving parts or stripping foils. The ion source is readily accessible for maintenance without disassembly of the accelerator and the electronics equipment is assembled in modular units for easy servicing. Finally, because the RFQ linac has the property of being a mass separator

(velocity filter), only a single charge-to-mass ion species ($^3He^+$) is accelerated, thus eliminating all contaminant beams.

The design dimensions of an RFQ specifically tailored for use with INRT is a 12 inch diameter by 33 inch long cylinder, which can be positioned in any orientation. It has a weight of only 200 lb. The grounded cylinder contains the ion source, extraction system, beam transport and focusing elements between the ion source and RFQ, and the RFQ resonator assembly. The ion source is a duoplasmatron operating with a diode extraction system at 25 kV. The ion source output is focused into the RFQ linac by using a single two-gap einzel lens.

The 23 inch long RFQ linac resonator is mounted inside the vacuum chamber. It operates at a frequency of 425 MHz and is less than 9 inches in diameter. The 425 MHz rf power is supplied by an air-cooled two stage amplifier employing compact grounded-grid planar triodes. The rf power system is conservatively rated at 40 kW of pulsed rf output, which is more than adequate for the INRT RFQ. The cooling and diagnostic signals for this system are fed through the end flange of the vacuum system. The rf power is fed through the vacuum chamber into the resonator using a coaxial cable that also goes through this end flange. The accelerator and injector are pumped by a turbomolecular pump that is mounted on the chamber through a flanged port. The cooling for the ion source and RFQ resonator is provided by a self-contained cooling system mounted within the electronics cabinet. The vacuum controls and roughing system are also mounted in the cabinet, which is a standard double bay cabinet of six foot height.

All of the remaining support electronics, including the rf power amplifier to drive the RFQ, are located within the electronics cabinet. This cabinet contains an isolated high voltage deck for the ion source power supplies and gas input system, the high voltage power supplies for the ion source, einzel lens and rf amplifier, and the control system. The cabinet is powered from a single 110V, single phase input at 20A maximum current and has a gross weight of less than 1500 lb. In this application, the accelerator is designed to be used remotely from the cabinet and can be mounted in any orientation. The accelerator is connected to the cabinet through a five inch diameter, flexible umbilical cable for all power and cooling. Similarly, the control computer and monitor can be connected remotely to the cabinet through a single twisted pair cable from the rack monitor and interface chassis.

The PC-based control system has two levels of operation. For routine operation, the high level enables even an unskilled operator to run the INRT RFQ with a fixed parameter configuration using only a few function keys. The individual control loops and accelerator diagnostics are available at the lower level, allowing a trained technician to optimize the beam parameters and change the beam pulsing characteristics.

The output beam has a diameter of 1.1. mm, but can be focused to a parallel beam of 1.0 mm diameter or it can be expanded to be 2.0 cm in diameter by using no focusing magnets. This makes the INRT RFQ ideally suited for use in either μINRT or Topical INRT. AccSys Technology, Inc. has also constructed a deuterium-beam RFQ accelerator, the Model DL-1 Linac [15], with a deuterium ion beam

output of 6-8 milliamps; this model could serve as a deuterium producing accelerator for the inverse nuclear reaction.

ii. Nested High Voltage Generator

The Nested High Voltage Generator (NHVG) is a compact DC accelerator technology which is well suited to the generation of ion beams in a "tandem" configuration. In an INRT tandem accelerator, a beam of positive ^{3}He ions is generated by a duoplasmatron ion source. These ions traverse a low density gas cell where a fraction of the ions (a few percent) undergo charge exchange to become negative ions. These ions are accelerated to an energy of 400 keV in the center of the accelerator. At that point, they strike a thin carbon foil which "strips" electrons from the negative ion, and it once again becomes a positive ion. The ion, having changed sign is now accelerated to ground potential through the second half of the tandem column. Some of the ions are actually doubly charged, and the beam which reaches ground potential consists of 800 keV and 1200 keV ions (minus 50 - 100 kV lost in the stripping foil).

The tandem accelerator must both produce voltage and insulate that voltage. The NHVG has a very small diameter, (less than 20"), owing to the use of solid dielectric insulation. Voltage is created in the NHVG using 8 individual 50 kV sections in series. These sections are "nested" inside each other to prevent fault modes from propagating between stages and damaging the insulation. The voltage is produced through transformer action - a primary coil couples magnetic flux to a secondary coil in each section, and that secondary, in turn, drives a voltage multiplier which increases the voltage and rectifies the voltage.

The NHVG will have a power consumption of less than 1 kW (plus vacuum pump power), and a length of about 30" including the vacuum system, target, ion source, and charge exchange cell. The length of the 400 kV NHVG by itself is approximately 20". The currents required are a few microamperes, so that ion beam optics considerations are not critically important. Ancillary equipment which can be housed in a rack at a convenient distance from the accelerator module includes a 200 kHz. oscillator (approximately 1 cubic ft.) and a control system (approximately 2 cubic ft.). The NHVG is well suited to INRT proton production due to it's small size, low cost, and low power consumption.

iii. INRT Targets

The d(^{3}He,p)^{4}He nuclear reaction can be induced with either a ^{3}He beam and deuterium target, or a deuterium beam and ^{3}He target. In using an 800 keV ^{3}He ion beam, the deuterium-containing target is easily fabricated and ^{3}He beam currents up to 1 milliamp can be achieved. If a deuterium ion beam is used with a ^{3}He target, the INRT accelerator can be somewhat smaller since the beam energy need only be 550 keV, but fabrication of a suitable ^{3}He target has not been demonstrated. However, there do exist material structures that show great promise as potential high concentration ^{3}He "solid" targets. Direct ion implantation of multiple energy helium into metal (Al, Au, Cu, Ni) and metal alloy matrices has been

shown to nucleate bubbles which contain helium in the gas phase that yield overall He concentrations of 20-30 atomic percent. These helium bubbles are of the order of 1000 Angstroms in diameter and retain the helium gas even at elevated temperatures [16,17,18]. Alternatively, silica aerogels fabricated with porousities exceeding 90% by volume [19] could be charged with ^{3}He gas and capped to prevent out-diffusion of the helium, thus serving as an excellent "solid" ^{3}He target for the INRT technique.

Ultimately, selection of an ion source-target material combination for INRT depends on the mode of use. For μINRT, a 1 microamp incident ^{3}He beam with a ZrD_2 target does not impose a limitation since, as shown in figure 3, accumulation of radiation damage is rapid. However, for topical INRT, where additional exposure area is achieved at the expense of a $1/r^2$ reduction in radiation intensity, higher beam currents may be desirable to increase dose rate. Though up to 1 milliamp ^{3}He currents can be produced by the RFQ-based INRT design, another option resides in the use of even higher output deuterium ion sources in conjunction with "solid" ^{3}He targets.

The prototype INRT needles fabricated and tested at Sandia National Labs used the ^{3}He/$ZrD_{1.9}$ beam-target combination; zirconium was used as the deuterated matrix solely for compatibility with on-going projects - as stated previously titanium, erbium, or scandium would serve as well. The body of the needles were fabricated from seamless stainless steel tube stock of 0.040", 0.135", 0.203", and 1.0" outer diameter. Deuterated target disks were fabricated for each of the selected tube diameters using the following procedure. Appropriately sized disks for each tube size were punched from .001" (25μ) and .005" (127μ) stainless steel foils and mounted in an electron-beam evaporator with a base pressure of $1x10^{-9}$ Torr. The substrate disks were heated to 350 °C until the chamber pressure recovered to better than $1x10^{-8}$ Torr. With deposition blocked by a shutter, the evaporator source was heated until the pressure recovered to better than $1x10^{-7}$ Torr. The shutter protecting the stainless steel disks was then retracted and a 5 micron of zirconium layer was deposited onto the disks; the circumference of each disk, which is later welded to the stainless steel tube, was masked to preserve a clean welding "lip". After deposition, the source was turned off and the pressure allowed to recover to $1x10^{-8}$ Torr. The zirconium-deposited disks were then heated to 500 °C for 15 minutes and then cooled to 350 °C. At this temperature, the evaporation chamber was back-filled with 10 Torr of deuterium gas for 15 minutes, after which the chamber was evacuated, the sample cooled, and removed. Measurements using the D(^{3}He,α)H deuterium profiling technique indicate typical stoichiometries of $ZrD_{1.9\text{-}1.95}$. Finally the deuterated discs were electron beam welded to the stainless steel needle stock with the deuterated layer facing inward. The needle is inserted into a swaged fitting that is welded into a 2.75" Conflat flange which, in turn, is mounted on the beamline of the EN Tandem Van de Graaf accelerator which provided the ^{3}He beams used for the radiation dose measurements. Free-standing thin metal zirconium foils (≈5μ) mounted in stainless steel frames are commercially available [20] and would be a suitable replacement for the evaporated films used here.

Medical Applications

i. μINRT

Radiation therapy is an effective treatment of neoplasms [21,22]. The goals of all modes of radiation therapy are to kill tumor cells and to minimize complications in the surrounding normal tissue. However, the utility of radiation therapy is limited by the difference between the radiosensitivity of the cancer cells and that of the surrounding normal tissues, since radiotherapy is most commonly administered via an external beam [23]. Complications of radiotherapy are defined as symptoms caused by death of normal tissue in the path of the beam. Curves relating the radiation dose to the probability of tissue death for either tumor tissue or nearby normal tissue are described in figure 6. The curve describing the probability of tumor tissue death represents the probability for cure of the tumor, while the probability of normal tissue death relates to the incidence of complications. Strategies for delivery of radiation therapy manipulate many factors in an attempt to maximize the separation of these two curves. This will maximize tumor control while minimizing complications for any specific dose level.

The strategies employed to minimize complications include manipulation of the size of each dose fraction, the treatment volume, the time between each fraction, and the total number of Grays of radiation administered. The complications result from the need to treat a tumor through normal tissue. Because radiotherapy is usually administered as an external beam, the field of tissue radiated includes the tissue between the radiation source and the tumor, the tumor itself and the tissue in the path of the beam but distal to the tumor. INRT has been developed to bypass the radiation effect on normal tissue that surrounds tumor tissue. By limiting the field of tissue receiving radiation and avoiding radiating normal tissue, much higher doses of radiation therapy can be given, ensuring that the tumor is eradicated, yet complications are minimized. These doses can be high enough that they are destructive to all tissues. With INRT the radiation field is small and can be precisely placed without the need for transmitting it through normal tissues, and the higher doses are absorbed almost exclusively by the tumor tissue. Also, for these reasons larger fractions can be given. This allows a tumor to be treated in a smaller number of fractions than with external beam radiation therapy (EBRT).

The prospective internal uses of INRT can be broken down into three broad categories: Treatment of tumors in difficult to reach areas; treatment of tumors that are situated near structures that are easily damaged by radiation therapy or surgery; and treatment of surgical margins. Tumors often occur in organs in which it is difficult to operate. The difficulties may be because the surgical approach is hazardous or because surgery on a particular organ is technically difficult. Although tumors often occur in the brain, the vast majority are situated deep in the parenchyma and not on the surface [24,25]. These tumors are not easy to resect because all the intervening brain tissue between the surface of the brain and the mass to be resected will be disrupted by the surgical approach. Similarly, all brain tissue in the path of external beam radiotherapy will be affected by the treatment.

These tumors can easily be biopsied using a stereotactic CT guided needle [24,25,26]. This allows a needle to be placed into an intracranial mass according to coordinates calculated from a pre-determined frame of reference. When the needle is passed into the mass, cells can be withdrawn to be analyzed by a pathologist. At this point, a second needle with a deuterated tip can be inserted into the mass and the lesion can be ablated using INRT. Because this approach is minimally invasive (a single burr hole through the skull followed by sequential passes with two different needles along the same line) the disruption to the brain is markedly reduced.

Early tumors of the kidney occupy the other end of the spectrum. The kidney has such a high blood flow rate that surgery on it is very difficult. If an attempt is made to remove only a portion of the kidney the intra-operative blood loss is very high, and the post-operative course has a high complication rate secondary to delayed bleeding [27,28]. Because of this, the usual treatment of a renal mass is removal of the entire kidney, which is a much safer procedure. With INRT the deuterated needle tip can be inserted into the mass percutaneously (through the skin, without any incision), the placement of the needle can be confirmed by ultrasound or CT scan then the mass can be treated with INRT. If the mass is larger than the treatment volume provided by INRT, this procedure can be employed repetitively. These treatments may be either at the same setting or serially. Other locations where these strategies can be employed include the thyroid and the lung.

The second category consists of tumors that have occurred near structures that would be no longer functional after surgery or EBRT, such as the eye or the vocal cords. Tumors of the vocal cords are readily cured by both surgery and EBRT [29], however the EBRT standard field is a 6x6 cm^2 area with all the attendant morbidity of radiating the skin, the entire larynx, a portion of the pharynx and cervical spinal cord that corresponds to the 6x6 cm^2 port. This can be avoided by using INRT. A needle can be placed on the lesion through an endoscope inserted through the mouth. The lesion can then be treated. It is unclear how the larynx will react to a single tumoricidal dose of INRT or if multiple smaller fractions will have to be administered. Those clinical studies will have to be performed to determine the normal tissue tolerance.

The third category is treatment of close surgical margins. There are many areas in the head and neck region where tumors occur in close proximity to structures that cause significant complications if resected, such as the carotid arteries, cranial nerves and the floor of the cranial fossa (the bone that separates the brain from the nasal sinuses). Tumors may be adjacent to these structures without invading them, nevertheless, the structures are at increased risk for harboring microscopic foci of the tumor [30,31,32]. This leads us to search for a modality to treat surgical margins (i.e. the edges of the resected areas). In the past external beam radio-therapy has been used post-operatively, but this causes all the side effects associated with EBRT and treats an entire anatomic region when treatment of only the resection margins are necessary. Some centers have employed intra-operative radiation (IORT) therapy to this end [31,32,33,34,35,36].

ii. Topical INRT

INRT could prove useful as a radiation source that could be brought directly into the operating theater for IORT procedures. In today's treatment arena, following surgical removal of large tumors within the abdominal cavity, many physicians prefer to irradiate the area which surrounded the tumor with a single dose of high energy electrons in order to kill remaining isolated tumor cells. Currently, IORT procedures typically require that after removal of the tumor, but before the surgical field (wound) has been closed, the patient be transported to radiation facilities outside the operating room, most often located in the hospital basement for shielding purposes. The patient is maintained on a ventilator under general anesthesia and transported to the radiation facilities along with the surgeon, anesthesiologist and operating room team. The wound, though sutured, is still open and at risk for infection. The additional risk to the patient, scheduling difficulties with radiation equipment, and the compounded complexity of the procedure could be vastly reduced if a small, portable radiation source could be brought into the operating room. Since INRT uses a compact, low power accelerator to produce localized high energy radiation, it could provide the surgeon with a rollaway system which could be wheeled into position and used to irradiate the tumor-bed with protons of a fixed penetration range. Additionally, the radiation administered will not have any significant range of penetration through underlying normal tissue and only the margins are treated. This should maximize the therapeutic effects while minimizing the complications of radiotherapy. This implementation of INRT would require a displaced source, as shown in figure 2b, to promote the radiation exposure over a large enough surface area. It should be emphasized that IORT, as yet, is not established to be of major benefit to patients and still represents a research effort. However, its potential in patients who are marginally resectable would appear obvious.

Another obvious application of the INRT technique involves its use in a doctor's office for dermatologic applications. The treatment of skin cancers, by using fractionated radiation treatments with INRT which could be delivered quickly to the affected region, could avoid procedures involving surgical removal or laser ablation, as well as their ensuing scarring, and minimize the requirement for elaborate radiation producing equipment. This would be especially true for melanoma, where conventional treatments with irradiation have been far less than ideal. An example of the broad area implementation of the INRT technique is illustrated in figure 2b where the radiation intensity patterns are shown for needle-to-tissue separations of 6". In this mode of usage, the retraction of the needle tip from the targeted area (i.e., displaced source) results in a widening of the affected area and a smoothing of the radiation dose distribution patterns. Thus, broad and uniform exposures are attainable for dermatologic applications of the INRT technique and potentially for lesions that are located in the brain and liver.

Conclusions

The concept of utilizing low energy, ion-induced nuclear reactions to produce radiation suitable for radiotherapy purposes has been described. One implementation of this concept, using the 650 keV

$d(^3He,p)^4He$ nuclear reaction, has been detailed with respect to the design and fabrication of the deuterated needle tips which, used in conjunction with a ^3He ion beam, produce 17.4 MeV proton radiation. The radiation dose patterns achievable with both an internal point-source and an external topical exposure have been calculated using a computer simulation incorporating the $1/r^2$ and Bragg peak effects on the delivered dose; comparison to experiment verifies the simulation. Thermal effects arising from internal use, as well as the design and availability of suitably compact, commercial ion accelerators and ion sources are also examined. Lastly, potential clinical applications of such a source of radiation have been commented on.

Developments in radiation therapy have historically stressed increasing dose control and localization of radiation damage. Advances in the design of novel radiation producing equipment, radiation delivery, and research in manipulating the radiosensitivity of tissue through chemical, thermal and other means will likely contribute to improved tailoring of the delivery of radiation damage. The use of low energy, nuclear reactions to produce highly localized, therapeutic radiation utilizing relatively inexpensive, compact, low-energy ion accelerators may contribute to specific modes of treatment. Moreover, the small size, reduced power requirements and support facilities of this technique make it conducive to use in the medical office or operating theater and may also provide efficient radiotherapy capabilities, (especially for melanomas), to the large Third World community which has a great need for affordable radiation treatment facilities.

ACKNOWLEDGMENTS

The authors would like to thank Scott Serano, Dave Walsh, Mike Selph, Sam Meyers, Jeff Brinker, and George Klody (NEC) for useful discussions, advice, and assistance in exploration of this topic.

Figure Captions

1. Energy deposition versus depth for several forms of radiation. Electron beams and x-rays display a broad region of energy deposition in which significant damage to healthy tissue can occur. High energy proton and deuteron beams, incident from outside the body, display sharp end-of-range damage peaks, but also do significant damage to healthy tissue along the incident path. 17.4 MeV protons, created at the site of the tumor using low energy, ion-induced nuclear reactions, irradiate a much more localized volume. An evacuated needle delivers the low energy ion beam to the site of the tumor, avoiding any radiation damage to healthy tissue.

2. Schematic representations of the INRT concept and resultant radiation damage. a) μINRT: An incident ion beam is directed down an evacuated needle to selected target material at the needle's end. The resulting dose-rate pattern is shown for a 1 μA, 800 keV ^{3}He exposure on TiD_2. (b) topical INRT: A broad beam irradiates a deuterated target displaced 6" from the treatment surface, thus exposing a wider area. The resulting dose-rate pattern is shown for a 1 mA, 800 keV ^{3}He exposure.

3. The time evolution of the accumulated damage deposited with the μINRT technique. Dose cross section curves are based upon use of a 1.0 μA , 800 keV ^{3}He beam on TiD_2 target needle.

4. Comparison of computer calculated dose and the measured energy deposition of protons produced by an INRT needle in a water target. The range of the INRT protons is reduced from 3.1 mm due to additional energy losses in the detector's surface metallization layer and waterproofing shroud.

5. Tissue heating induced by μINRT. Time-dependent temperature profiles are shown for positions 0, 3, and 5 millimeters away from the needle tip during a 100 second μINRT exposure using an incident 1 μA, 800 keV ^{3}He ion beam.

6. Dose-response curves for control of a hypothetical tumor and for normal tissue damage. Treatment to dose level 1 results in a 90% probability of cure and 10% probability of complications. Because of the shape of the sigmoid response curves, if the dose is increased to level 2, the control rate increases by only 5% but the rate of complications increases more dramatically to 28%. The actual separation between the two curves will vary for different treatment regimens and tumors types.

REFERENCES

[1] G.T.Y. Chen, J.R. Castro, and J.M.Quivey, Ann. Rev. Biophys. Bioeng., Vol. 10, 1981, pp. 499-529.

[2] PARTICLES Newsletter. Number 11, January 1993.

[3] R.R.Wilson, Radiology, 47, 487-491 (1946).

[4] G.L.Locher, Am. J. Roentgenol., 36:1 (1936).

[5] K.M.Horn and W.A.Lanford, Nucl. Instr. and Meth. B34 (1988) pp. 1-8.

[6] Möller and F. Besenbacher, Nucl. Instr. and Meth. 168 (1980) pp. 111-114.

[7] TRIM-88, computer code by J.F. Ziegler, IBM-Research, Yorktown Heights, NY 10598.

[8] M.Tubiana, J.Dutreix and A. Wambersie, Introduction to Radiobiology, (Taylor & Francis, London, 1990). p. 256.

[9] Gozani, T, Nucl. Instr. and Meth. B79 (1993) pp. 601-604.

[10] W.D.Cornelius and P.E.Young, Nucl. Instr. and Meth. B79 (1993) pp. 933-935.

[11] J.E. Stovall, K.R. Crandall and R.W. Hamm, IEEE Trans. Nucl. Sci. NS-28, No. 2 (1980) 19.

[12] H. Klein, IEEE Trans. Nucl. Sci. NS-30, No. 4 (1983) 3313.

[13] S.O. Schriber, IEEE Trans. Nucl. Sci. NS-32, No. 5 (1985) 3134.

[14] K.R. Crandall, R.H. Stokes and T.P. Wangler, Proc. 1979 Linac Conf., BNL-51134 (1979) 205.

[15] R.W. Hamm, J.H. Bower, K.R. Crandall, M.E. Hamm, and J.M. Potter, Proc. European Particle Accelerator Conf. (World Scientific, June 1988) 1462.

[16] W. Jäger and J. Roth, Nucl. Instr. and Meth. 182/183 (1981) 975-983.

[17] P.B.Johnson and D.J.Mazey, Radiation Effects, 1980, Vol. 53, pp. 195-202.

[18] W.Jäger, R.Manzke, H.Trinkaus, G.Crecelius, R.Zeller, J.Fink, H.L.Bay, J. of Nucl. Matls. 111 & 112 (1982) 674-680.

[19] T.M.Tillotson and L.W.Hrubesh, Jour. of Non-Crystalline Solids 145 (1992) 44-500.

[20] Lebow Co., Goleta, CA 93117.

[21] Management of Head and Neck Cancer: A Multidisciplinary Approach, (J.B. Lippincott Company, Philadelphia).

[22] Maran, A.G.D., Gaze, M., Wilson, J.A., Stell and Maran's Head and Neck Surgery, (Butterworth/Heinemann).

[23] Management of Head and Neck Cancer: A Multidisciplinary Approach, (J.B. Lippincott Company, Philadelphia), pp. 299-309.

[24] Thomas, D.G., Kitchen, N.D., British Medical Journal, 1994, Jan. 8, Vol. 308, Issue 6921, pp. 126-128.

[25] Gomez, H., Barnett, G.H., Estes, M.L., Palmer, J., Magdinec, M., Cleveland Clinical Journal of Medicine, 1993, Sept.-Oct., Vol. 60, Issue 5, pp. 399-410.

[26] Levivier, M., Goldman, S., Pirott, B., Brotchi, J., Acta Neurologica Belgica, 1993, Vol. 93, Issue 1, pp. 5-22.

[27] Taari, K., Salo, J.O., Rannikko, S., Nortling, S., Lasers in Surgery and Medicine, 1994, Vol. 14, Issue 21, pp. 21-26.

[28] Thrasher, J.B., Robertson, J.E., Paulson, D.F., Urology, 1994, Feb., Vol. 43, Issue 2, pp. 160-168.

[29] Maran, A.G.D., Gaze, M., Wilson, J.A., Stell and Maran's Head and Neck Surgery, (Butterworth/Heinemann), pp. 114-118.

[30] Management of Head and Neck Cancer: A Multidisciplinary Approach, (J.B. Lippincott Company, Philadelphia), p. 72.

[31] Willett, C.G., Lewandrowski, K., Warshaw, A.L., Efird, J., Compton, C.C., Annals of Surgery, 1993, Feb., Vol. 217, Issue 2, pp. 144-148.

[32] Pelton, J.J., Lanciano, R.M., Hoffman, J.P., Hanks, G.M., Isenberg, B.L., Journal of Surgical Oncology, 1993, May, Vol. 53, Issue 1, pp. 30-35.

[33] Shibamoto, Y., Yamashita, J., Takahashi, M., Abe, M., American Journal of Clinical Oncology, 1994, Oct., Vol. 17, Issue 5, pp. 396-399.

[34] Pass, H.I., Annals of Thoracic Surgery, 1994, Jul., Vol. 58, Issue 1, pp.269-270.

[35] Zerbi, A., Fossati, V., Parolini, D., Carlucci, M., Balzano, G., Bordogna, G., Staudacher, C., DiCarlo, V., Cancer, 1994, June 15., Vol. 73, Issue 12, pp. 2930-2935.

[36] Close, L.G., Morrish, T.N., Nguyen, P., Laryngoscope, 1993, Mar., Vol. 103, Issue 3, pp. 231-246.

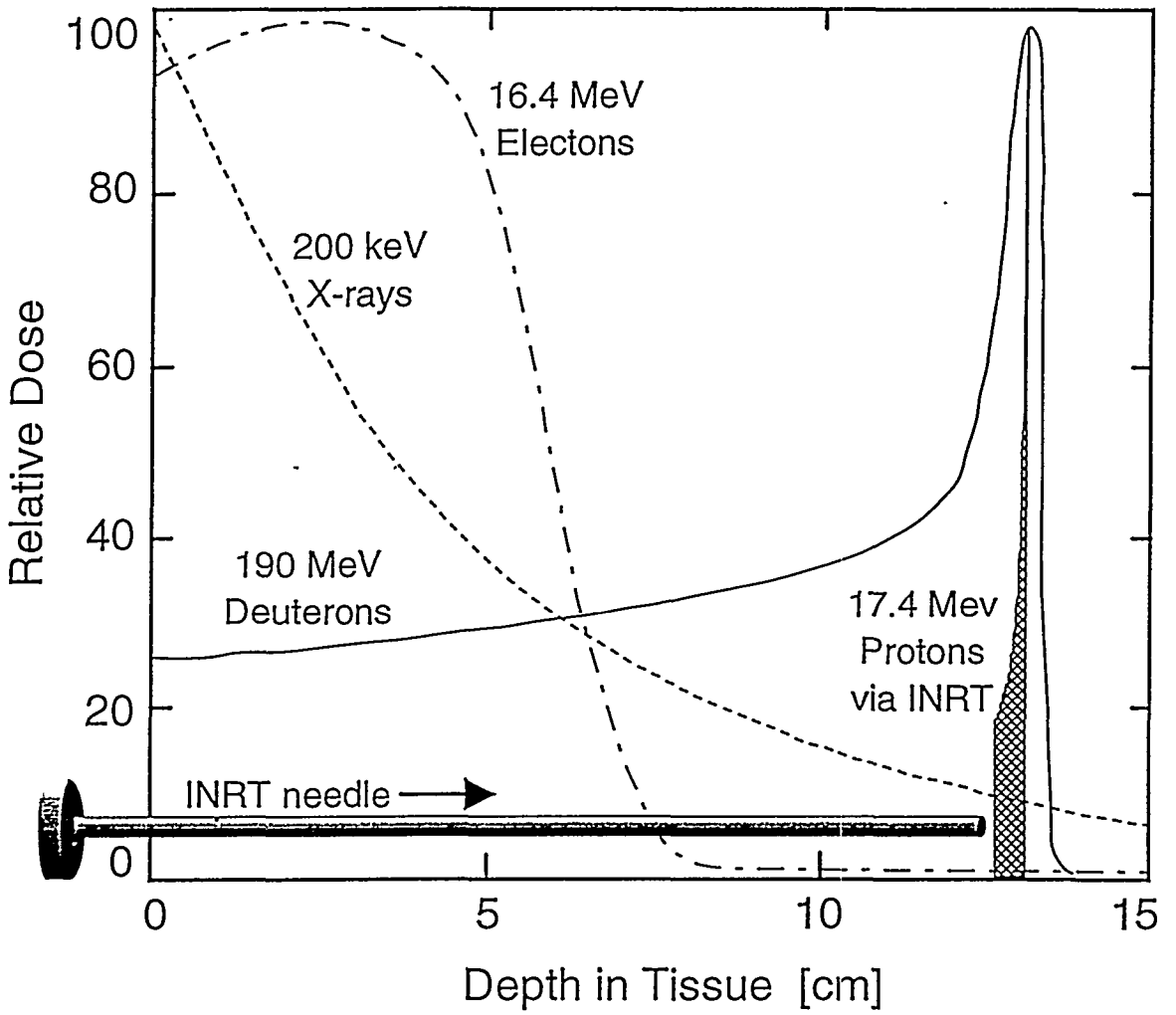
100
80
60
40
20
0
Relative Dose
16.4 MeV
Electons
200 keV
X-rays
190 MeV
Deuterons
17.4 Mev
Protons
via INRT
INRT needle
0
5
10
15
Depth in Tissue [cm]

Fig. 1

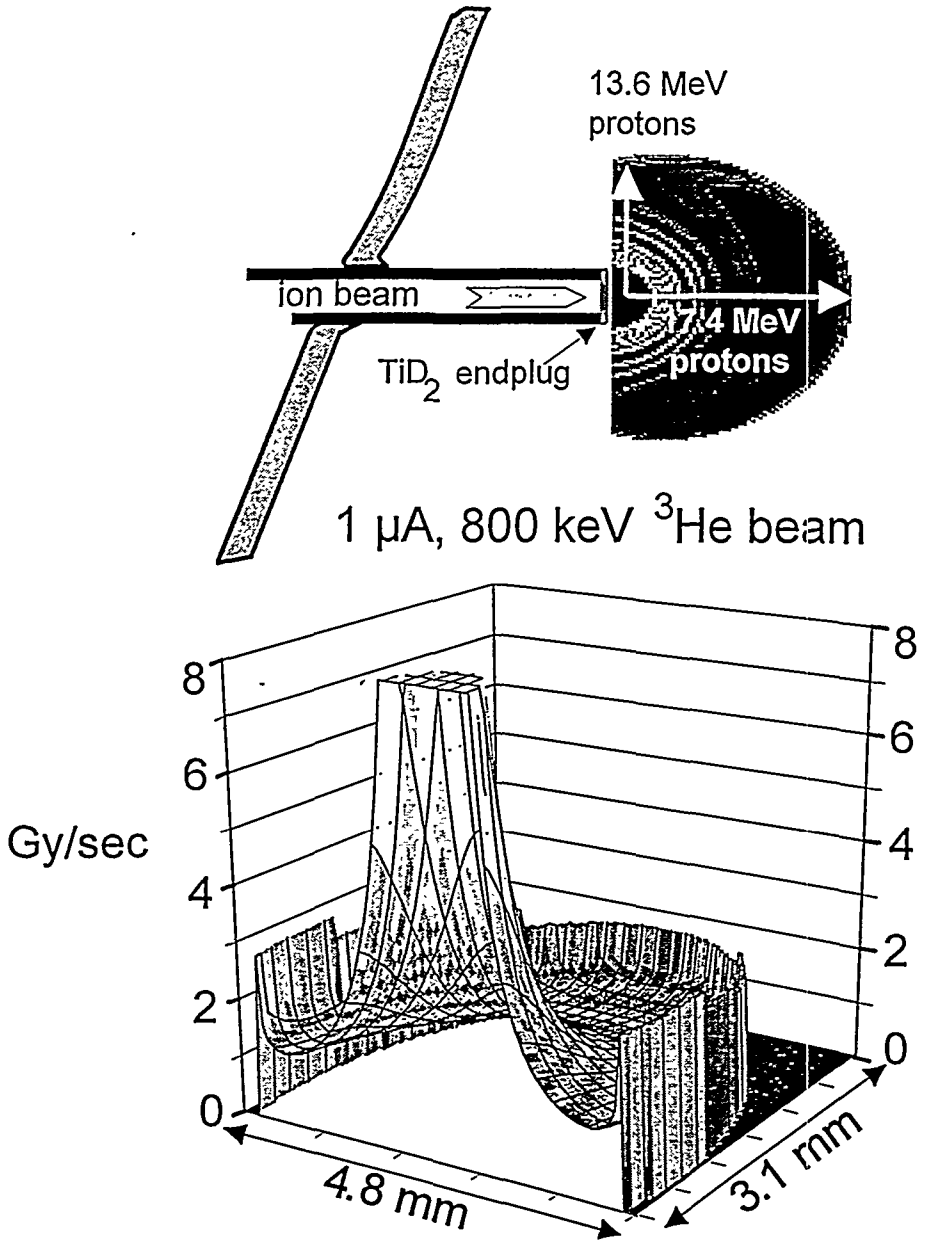

μINRT

Fig. 2 - left side

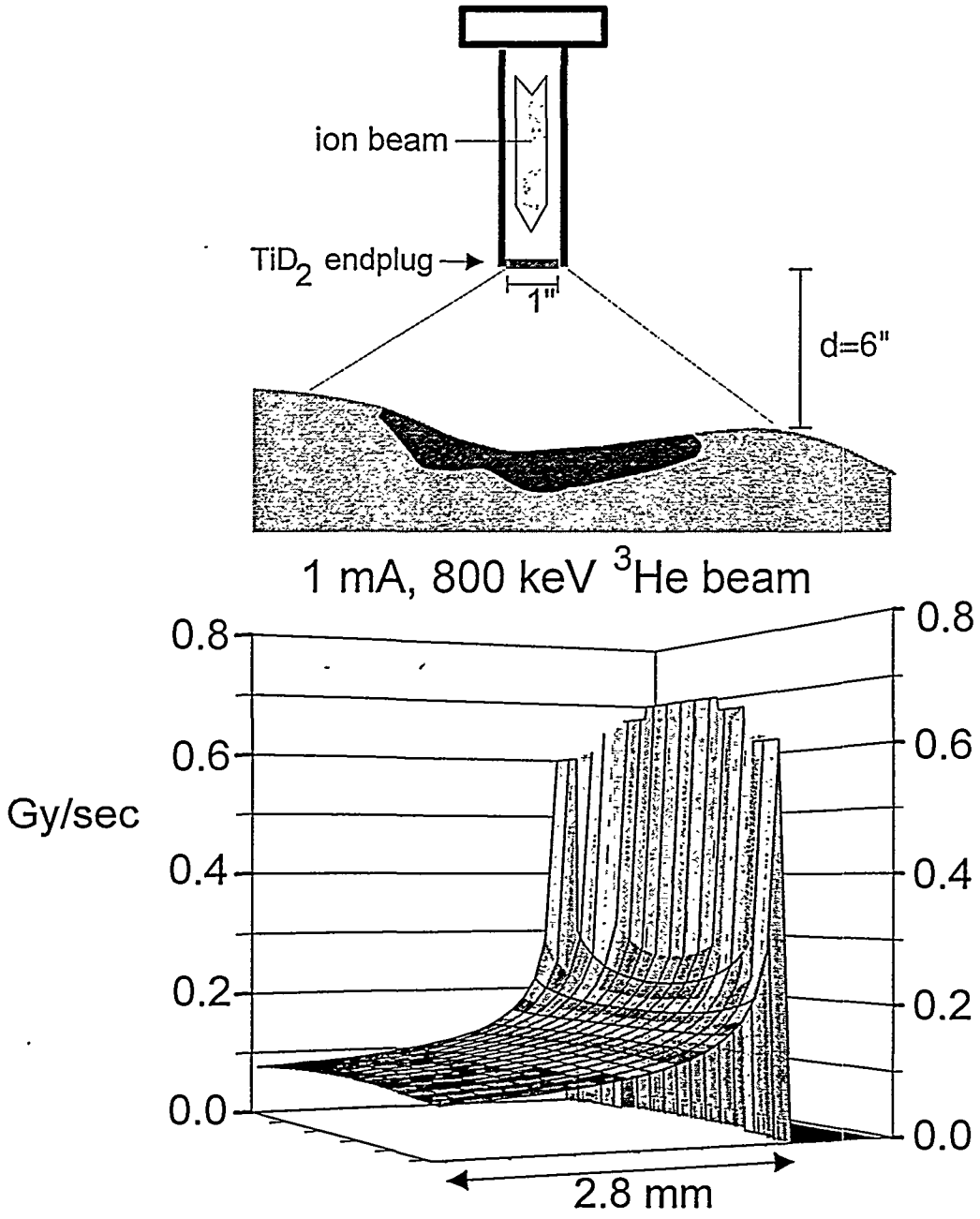

Fig. 2 - right side

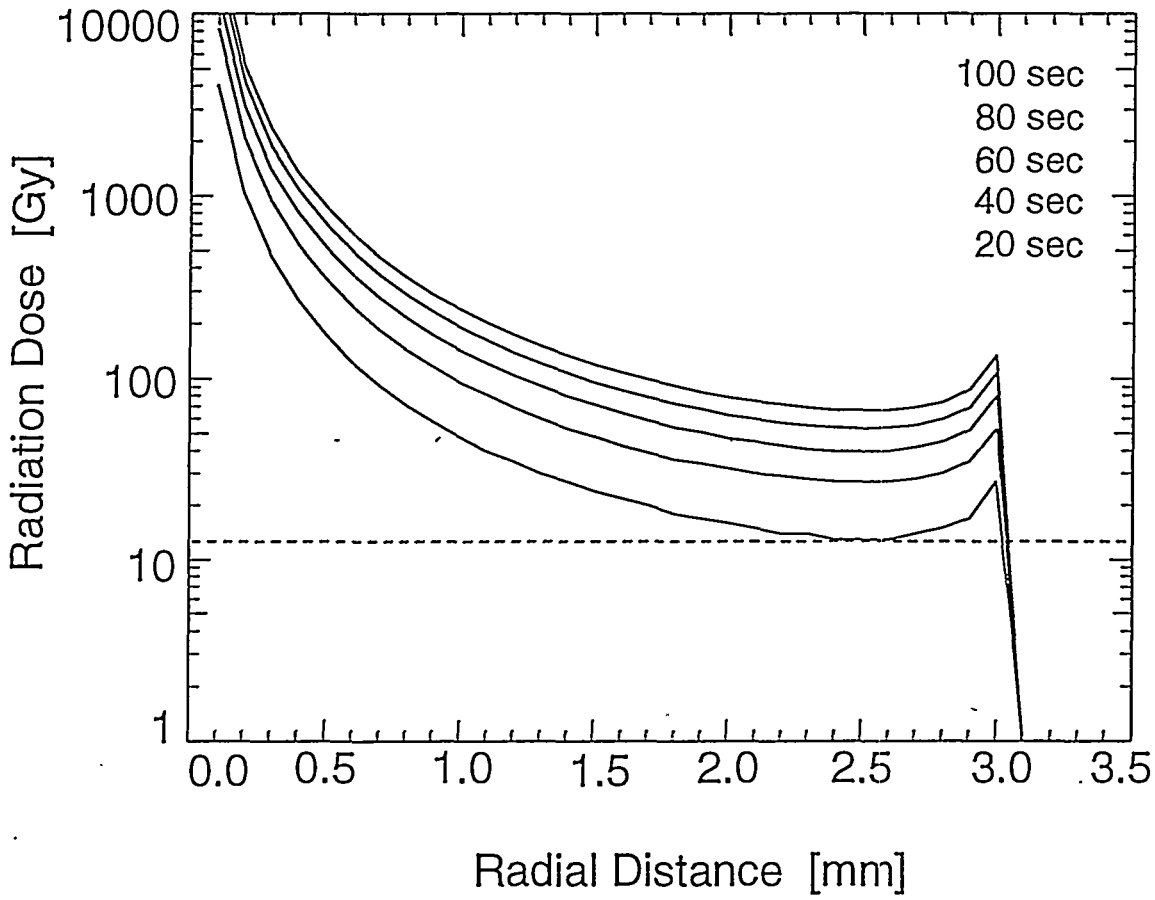
10000
1000
100
10
1
Radiation Dose [Gy]
100 sec
80 sec
60 sec
40 sec
20 sec
0.0
0.5
1.0
1.5
2.0
2.5
3.0
3.5
Radial Distance [mm]

Fig. 3

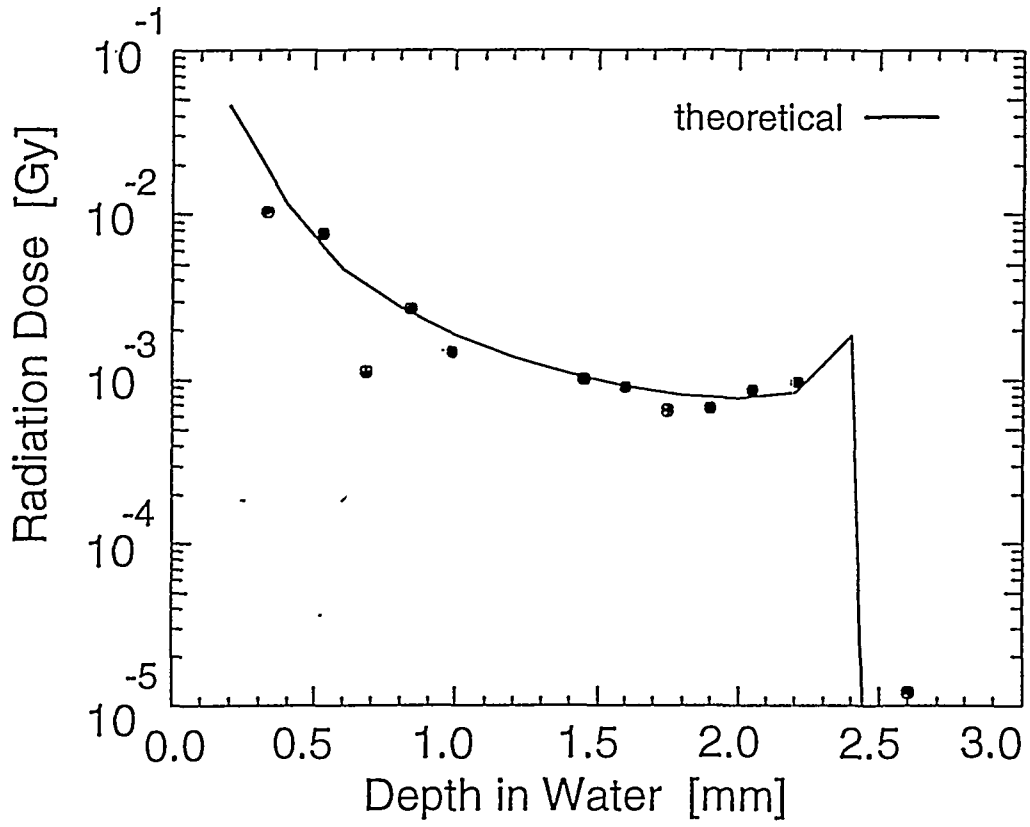
Radiation Dose [Gy]
10^-1
10^-2
10^-3
10^-4
10^-5
theoretical
0.0
0.5
1.0
1.5
2.0
2.5
3.0
Depth in Water [mm]

Fig. 4

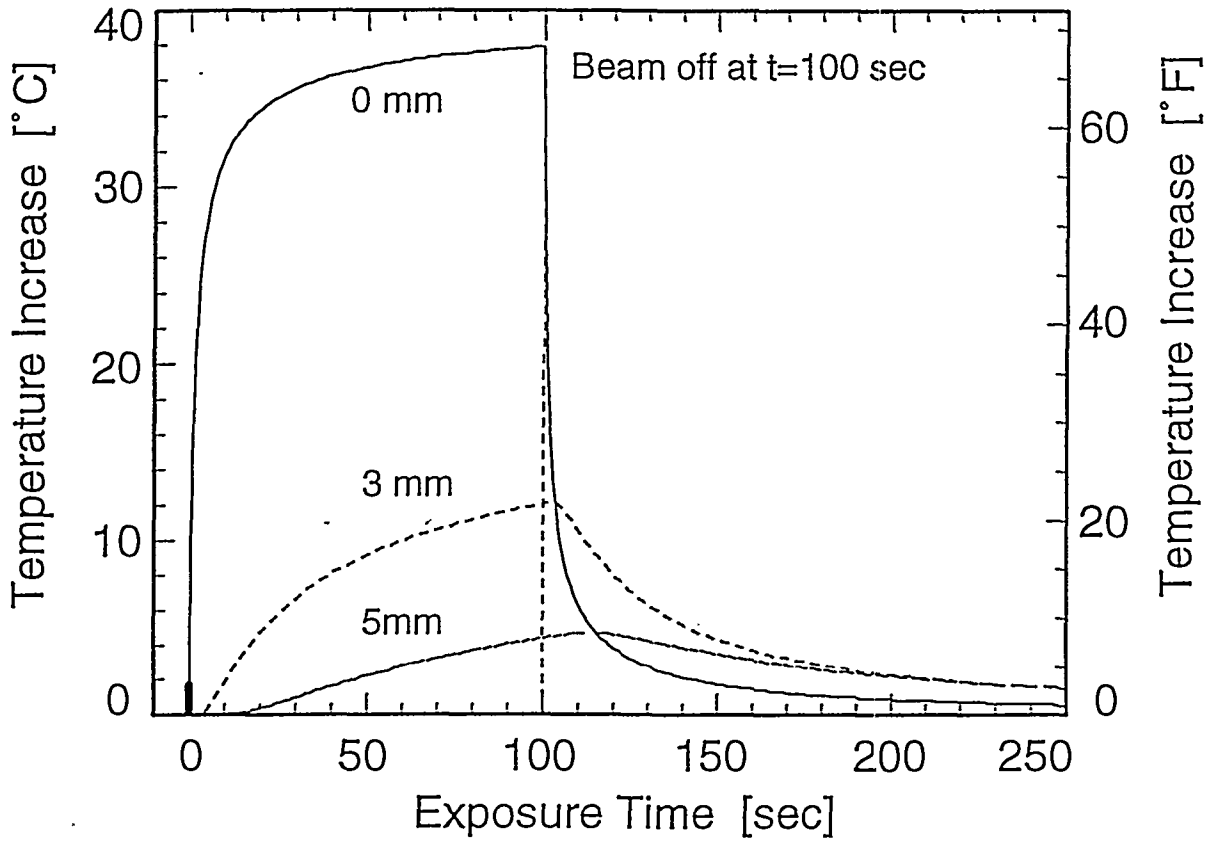
Temperature Increase [°C]
Temperature Increase [°F]
Beam off at t=100 sec
0 mm
3 mm
5mm
Exposure Time [sec]
0
10
20
30
40
0
20
40
60
0
50
100
150
200
250

Fig. 5

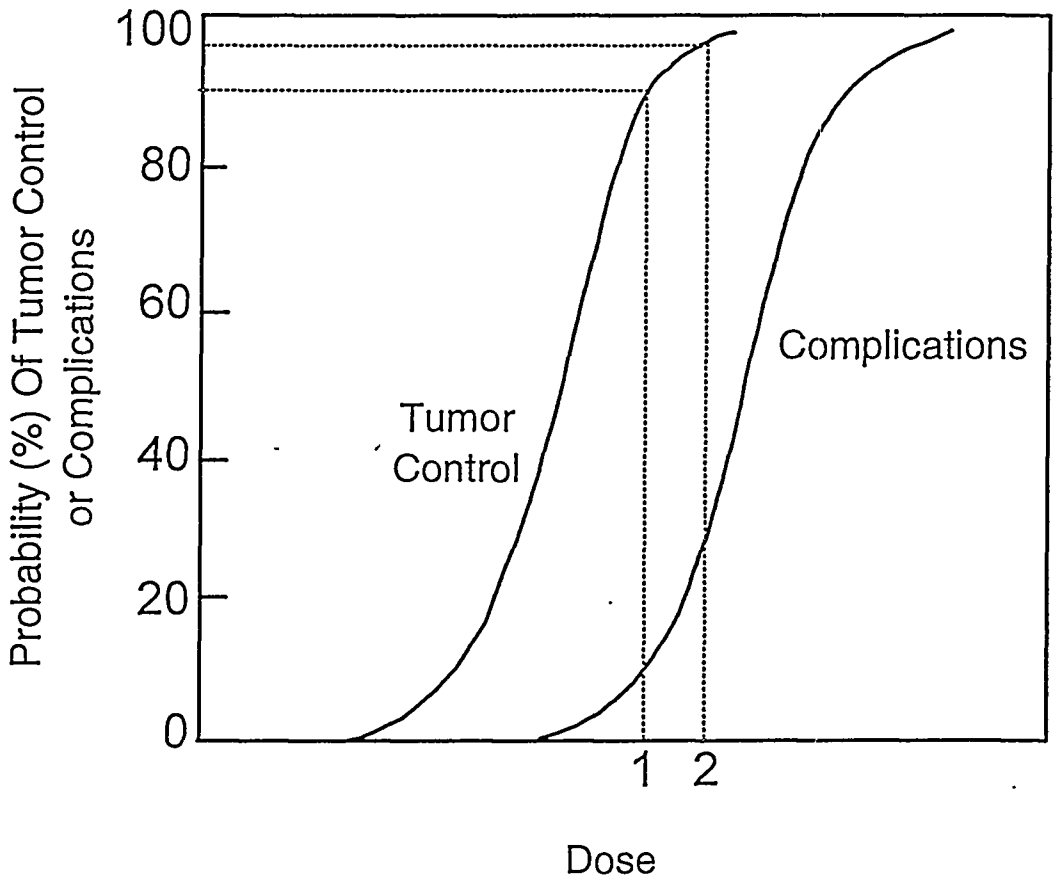
100
80
60
40
20
0
Probability (%) Of Tumor Control or Complications
Tumor Control
Complications
1
2
Dose

Fig. 6